MAPPING THE GREENNESS OF SEMI-ARID RANGELAND VEGETATION IN NORTHERN KENYA FROM LANDSAT DIGITAL DATA

G.H. Griffiths, Post graduate,
W.G. Collins, Reader,
University of Aston in Birmingham,
U.K.

1. Introduction

More than half of the land surface of Kenya with an annual rainfall of less than 600mm is classified as semi-arid and supports only a sparse shrub and grassland vegetation. This marginal grazing land in Kenya and across much of the Sahel zone of sub-Saharan Africa, has traditionally been used by pastoralists to support their herds of livestock. In recent decades recurrent drought combined with pressure upon grazing land from increased herd sizes, has in many areas resulted in a loss of rangeland productivity leading to widespread desertification (United Nations, 1977).

The primary objective of the research described here has been to identify the problems involved in mapping semi-arid vegetation in Northern Kenya from Landsat multi-spectral scanner (MSS) digital data, and to develop a methodology for monitoring changes in rangeland productivity. The area selected for the investigation is part of a larger region at present being studied by the United Nations Integrated Project for Arid Lands (IPAL). One of the aims of the IPAL project is to gather base-line data to serve as a reference point against which to measure ecological change (Lamprey, 1978). It was felt that the multi spectral, repetitive and synoptic coverage of Lansat data could provide timely and useful information on rangeland productivity.

The study area of approximately 600 km^2 lies to the east of Lake Turkana within a flat sedimentary basin of predominantly sandy/silty loam soils. In such an area of low and unreliable rainfall (<150mm/annum) (Edwards et al., 1979) the rangeland is of 'low potential, the vegetation being dwarf shrub grassland and a very dry form of bushed grassland, in which Acacia reficiens is a characteristic species' (Pratt et al., 1966). A green 'flush'of vegetation accompanies the wet season but towards the end of the rains green vegetation rapidly begins to senesce as the deciduous shrub and dwarf shrub species lose their leaves and the herbaceous layer begins to dry back.

2. Ground cover.

Within this semi-arid rangeland of Northern Kenya there are three major ground cover components, bare soil, non-green shrub and dwarf shrub, and green herbaceous vegetation (Herlocker, 1979). The percentage cover of each of these components within the study area was determined from twenty small format (35mm) vertical colour photographs each with a ground area of 6ha and taken from an altitude of 500m along six transects covering 200km^2. A 0.5ha grid containing one hundred evenly spaced dots was used to estimate the percent cover of each component. Five measurements were made on each photograph and the percentage cover was estimated by counting the number of dots falling on a particular cover type. Unavoidably the survey to collect ground data was flown two years after the date of the latest available Landsat scene for Northern Kenya (02 June 1979), and it is assumed that the ground cover had not changed substantially during the two intervening years of near normal rainfall.

3. Results.

MSS image data from a Landsat 2 scene taken on 02 June 1979 following a period of relatively high rainfall, was displayed as 2-dimensional scatterplots on an Interactive Image Analysis System for all pixels within the study area. The contoured plots are given in Figure 1, and show that the shape of the data cluster is approximately triangular for the #7/#5, #7/#4, #6/#5 and #6/#4 Landsat waveband combinations, with the soil line forming the base of the distribution. As the greenness of the vegetation cover increases pixels move away from the soil line (Kauth and Thomas, 1976), so that the point of high green cover is at the apex of the triangle, an effect due to the high spectral contrast between visible and infrared reflectance from green vegetation. Graetz et al. (1982) have similarly shown that for semi-arid vegetation in Central Australia, the shape of the #7/#5, #7/#4, #6/#5 and #6/#4 Landsat data space is essentially triangular due to high infrared reflectance and low visible reflectance from green ephemeral vegetation. By contrast, the elliptical distribution of points clustering close to the soil line in both #7/#6 and #5/#4 space (e-f), is indicative of a high correlation between the two infrared wavebands and between the two visible wavebands commonly observed for agricultural targets in middle latitudes.

In the model discussed below the distribution of reflectance in #7/#5 space is explained as being the product of a 3-component model whose 'end-points' are average reflectances for 100 percent bare soil, for 100 percent non-green shrub vegetation and for 100 percent green ephemeral herbaceous cover. The positions of each of these end-points in #7/#5 space were estimated by sampling Landsat #7/#5 reflectances for areas known from field-data and aerial photography to be bare soil, dense non-green shrub and green herbaceous cover (Table 1). The sampled #7/#5 reflectance values used to determine the position of each end-point are plotted in Figure 3 to show the scatter of points about the mean end-point values.

Table 1. Mean reflectance values and standard deviations for 100 percent bare soil, 100 percent non-green and 100 percent green vegetation in Landsat #7 and #5.

	Landsat #7	Landsat #5
100 percent bare soil	56 $\pm$6.2	79 $\pm$11.4
100 percent non-green shrub vegetation	32.5 $\pm$5.3	36 $\pm$6.6
100 percent green herbaceous vegetation	39.5 $\pm$3.8	36 $\pm$5.9

The soil line shown in Figure 3 is the least squares regression line for the reflectance of twenty bare soil pixels sampled within the study area. The figure shows that reflectance from soil is highly correlated in #7/#5 space (r^2 = 0.94), but that the spectral response of different soil types, which include sandy-loam, lava pebble and calcareous surfaces, and badly eroded soils, is somewhat variable. However, the majority of the study area is covered by a sandy-loam soil with a

relatively high and uniform response. The concept of a soil end-point is thus a reasonable one, and reflectance values from this soil type were therefore used to obtain an average reflectance for 100 percent bare soil in #7/#5 space.

The estimated end-point position of a 100 percent cover of non-green vegetation lies slightly above the 95 percent confidence limits for the soil line (Figure 2). It seems likely that the reflectance values used to estimate this point included some areas of green cover, either from an herbaceous ground layer beneath an open shrub canopy or from remaining green shrubland leaves. The effect of this would be to increase #7 reflectance and move the non-green point slightly above the soil line. However, it is believed that a 100 percent cover of completely non-green vegetation would be spectrally inseparable from bare soil (Siegal and Goetz,1977), and for the purposes of the model the non-green point is placed at the nearest point on the soil line.

In order to estimate the end-point position of maximum green cover, the image data was contrast stretched and pixels of high #7 and low #5 reflectance values were sampled. In the absence of field-data at the time of the Landsat pass, it has to be assumed that pixels of high #7 and low #5 reflectance corresponded to areas of maximum green cover within the study area. The shape of the scatterplots (Figure 2 a-d) fits closely with the distribution of the three end-points in the Landsat data space, suggesting that the assumption is a reasonable one. It is believed that at the time of the Landsat pass (02 June 1979) the only green vegetation remaining in the rangeland was herbaceous ephemerals and annual grasses. Although rainfall had been relatively high from the latter part of 1978 until the end of the wet season in April 1979, May was a dry month (0.7 mm), so that by 02 June the deciduous shrub layer would be almost without green leaves, leaving only the herbaceous layer still in green growth.

At the spatial resolution of the Landsat MSS scanner, total reflectance from a sparsely vegetated surface is an addition of reflectance from all components within a pixel (Bentley et al. 1976). From Figure 2 the reflectance of non-green vegetation with a DN (digital number) value of 31 in #7 and 20.5 in #5 is a significant component of a combined response from both soil and vegetation (Griffiths and Collins, 1982). In general an increase in percentage cover results in a movement down the 'cover-line' (Graetz et al. 1982), which in this case is thought of as joining the point of 100 percent bare soil with high reflectance, to the point of 100 percent non-green vegetation with low reflectance.

With the addition of a 'green' component the distribution of points in #7/#5 space for the 3-component model is determined by the relative proportions of bare soil, non-green and green vegetation within each Landsat pixel. Canopy cover measurements taken from the colour aerial photography were used to determine the percentage cover of non-green shrub against green herbaceous vegetation. In areas of low non-green shrub cover, green herbaceous cover is high and vice versa (Table 2). The vegetation is sparse however, and does not generally exceed 60-70 percent cover, with bare soil contributing between 30-40 percent of the total. The percentage figures for the varying proportions of bare soil, non-green and green cover represent distances along the 3 vectors, X, Y and Z respectively as indicated on Figure 4. By vector addition the position of a pixel can thus be plotted within the triangular

distribution of the Landsat data space. The four points plotted in Figure 5 represent pixels of high (> 60%), moderate (40-60%), low (20-40%) and sparse (< 20%) green cover determined from the colour air photography (Table 2). In general, with a decrease in the percentage cover of green herbaceous vegetation plotted points move down towards the soil line and away from the point of 100 percent green cover.

Table 2 Varying percentage of soil, non-green shrub and green herbaceous vegetation estimated from colour air photographs

Soil	Non-green shrub cover	Green herbaceous cover	'Greenness index'
40	50	10	Very low
40	40	20	Low
35	25	40	Moderate
30	10	60	High

In terms of the 3-component model, pixels of equal green cover lie on lines parallel to the soil line, but their positions on any such line will be determined by the percentage of bare-soil and non-green vegetation within the pixel. The percentage of bare soil remains fairly constant, ranging from 30-40 percent of the total, so that movement along a line of equal green cover mostly results from variations in the percentage cover of non-green vegetation. A decrease in non-green cover moves pixels up the soil line towards the 100 percent bare soil points, whilst an increase in non-green cover moves pixels in the opposite direction towards the point of 100 percent non-green cover. Thus the distribution approximates to the triangular data shape displayed in Figure 2 a-d, as pixels of varying green cover depart from the soil line at various points along it.

4. Image Analysis

A number of spectral ratio measure have been developed for mapping green vegetation, and it has been shown that these correlate well with measured parameters of the vegetation cover, including leaf area index (Curran, 1982), and biomass (Tucker, 1979). The simple #7/#5 ratio is one of these measures in which ratio lines of equal green response radiate from the origin at different slopes. In the 3-component model described above however, lines of equal green response lie parallel to the soil line. A measure of green vegetation cover is therefore represented by perpendicular distance from the soil line.

Richardson and Wiegand (1977) developed the perpendicular vegetation index (PVI) and difference vegetation index (DVI), both of which are relative measures of green vegetation amount e.g. biomass, perpendicular to the soil line. An index similar to the PVI was used in this study to calculate both distance along the soil line as a measure of the percentage non-green vegetation cover, and perpendicular distance away from the soil line as a measure of green vegetation cover:

distance along soil line = $MSS5\cos\theta+MSS7\sin\theta$

perpendicular distance along green vegetation line = $MSS7\cos\theta-MSS5\sin\theta$

where θ is the angle between the soil line and the x axis.

This is equivalent to a rotation of axes, such that in the new coordinate system the soil line becomes the abissca and the perpendicular vegetation line the ordinate. The method is similar to a principal components transformation with the soil line representing the first principal component and the vegetation line the second component.

The tranformation was applied to #7 and #5 image data over an extensive area of rangeland (2500 km^2) which included the study area, and the results displayed on an Interactive Image Analysis System as a green vegetation index image. Four types of cover were displayed on the image based upon a scaling of the perpendicular distance along the green vegetation line into four equal divisions. Areas of high green cover with high values at maximum distance from the soil line appeared bright on the image. Areas of lava, bare soil and non-green shrubland with low values at minimum distance from the soil line, appeared black on the image. Between these two extremes lie areas of medium green cover and low green cover displayed as light and medium grey tones respectively. The categories appeared to correlate well with a vegetation map interpreted from 1:50 000 scale black and white aerial photography and with a smaller scale (1:500 000) vegetation map produced by IPAL (Herlocker, 1979). In particular, areas of high green cover correspond with the distribution on the vegetation map of green Acacia tortilis/ Salvadora persica woodland, and with areas of open shrubland where the cover of green herbaceous vegetation is at a maximum.

The method was also applied to multi-temporal imagery to map variations in green cover between a dry season Landsat scene taken in January 1973 during the Sahel drought (1968-76), and the 'wetter' 1979 scene. The two maps were geometrically corrected and registered together before subtracting one image from another to produce a 'difference' image. The 'difference' image clearly showed the 'wetter' 1979 image to be considerably more green than the dry season 1973 image, suggesting that this method could be successfully applied to monitoring differences in the greenness and productivity of the rangeland over time.

5. Conclusion

It appears that reflectance in the infrared and visible wavebands from semi-arid vegetation in Northern Kenya can be described in terms of a 3-component model within which pixels containing varying proportions of bare soil, non-green shrub and green herbaceous vegetation are distributed in an approximately triangular fashion. The understanding gained from the model was useful in formulating the design of an image processing technique capable of mapping spatial and temporal differences in the greenness of the vegetation cover between a dry-season and immediately post wet-season Landsat scene. However, the model represents a simplified description of the reality and further fieldwork, including radiometric measurements and vegetation canopy cover sampling, will be required to calibrate the green vegetation index as a precise measure of vegetation greenness in order to monitor spatial and temporal differences in rangeland productivity resulting from both variations in rainfall and grazing intensity.

References

BENTLEY, R.G., B.C. Salmon-Drexler, W.J. Bonner, and R.K. Vincent, 1976: A Landsat study of Ephemeral and Perennial Rangeland Vegetation & Soils. NASA Report YA-300-1700-1012, Bureau of Land Management, U.S. Department of Interior, Denver, Colorado, 234 pp.

CURRAN, P.J., 1982: Multispectral Remote Sensing for Green Leaf Area Index Estimation, paper presented at a Royal Society Discussion Meeting, The study of the ocean and land surface from satellites, 28pp.

EDWARDS, K.A., C.R. Field, and I.G.G Hogg, 1979: "A Preliminary Analysis of Climatological Data from the Marsabit District of Northern Kenya. IPAL Technical Paper B - 1, (UNEP-MAB Integrated Project in Arid Lands), 44 pp.

GRAETZ, R.D. and M.R. Gentle, 1982: the Relationship Between Refelectance in the Landsat Wavebands and the Composition of an Australian Semi-arid Shrub Rangeland. Photogrammetric Engineering and Remote Sensing, Vol. 48, pp1721-1730.

GRIFFITHS, G.H., and W.G. Collins, 1982: Mapping Semi-arid Vegetation in Northern Kenya from Landsat Digital Data, Proceedings of I.S.P. Conference, Toulouse, September, 1982, pp 381-386.

HERLOCKER, D.J., 1979: Vegetation of Southwestern Marsabit District, Kenya. IPAL Technical Paper D - 1, (UNEP-MAB Integrated Project in Arid Lands), 65 pp.

HIELKEMA, Jelle U., 1980: Remote Sensing Techniques and Methodologies for Monitoring Ecological Conditions for Desert Locust Population Development, F.A.O. Technical Report, 63pp.

KAUTH, R.J. and G.S. Thomas, 1976: The taselled cap - a graphic description of the spectral-temporal development of agricultural crops as seen by Landsat, in Proceedings Symposium on Machine Processing of Remotely Sensed Data, Purdue University, pp 41-51.

LAMPREY, H., 1978: The Integrated Project on Arid Lands (IPAL). Nature and Resources, XIV4, pp 2 - 11.

PRATT, D.J., P.J. Greenway, and M.D. Gwynne, 1966: A classification of East African rangeland. Journal Applied Ecology, 3, pp 369-382.

RICHARDSON, A.J. and C.L. Wiegand, 1977: Distinguishing Vegetation from Soil Background Information, Photogrammetric Engineering and Remote Sensing, Vol. 43, pp 1541-1552.

SIEGAL B.S., and A.R.H. Goetz, 1977: Effect of Vegetation on Rock and Soil Type Discrimination. Photogrammetric Engineering and Remote Sensing, 43 No 2, pp 191 - 196.

TUCKER, C.J., 1979: Red and Photographic Infrared Linear Combinations for Monitoring Vegetation, Remote-Sensing of the Environment, Vol 8, pp 127-150.

UNEP, Desertification: Its Causes and Consequences, 1977, Compiled and edited by the secretariat of the United Nations Conference on Desertification, Nairobi, Pergamon, pp228.

Figure 1. Two-dimensional scatterplots for all possible Landsat waveband combinations.

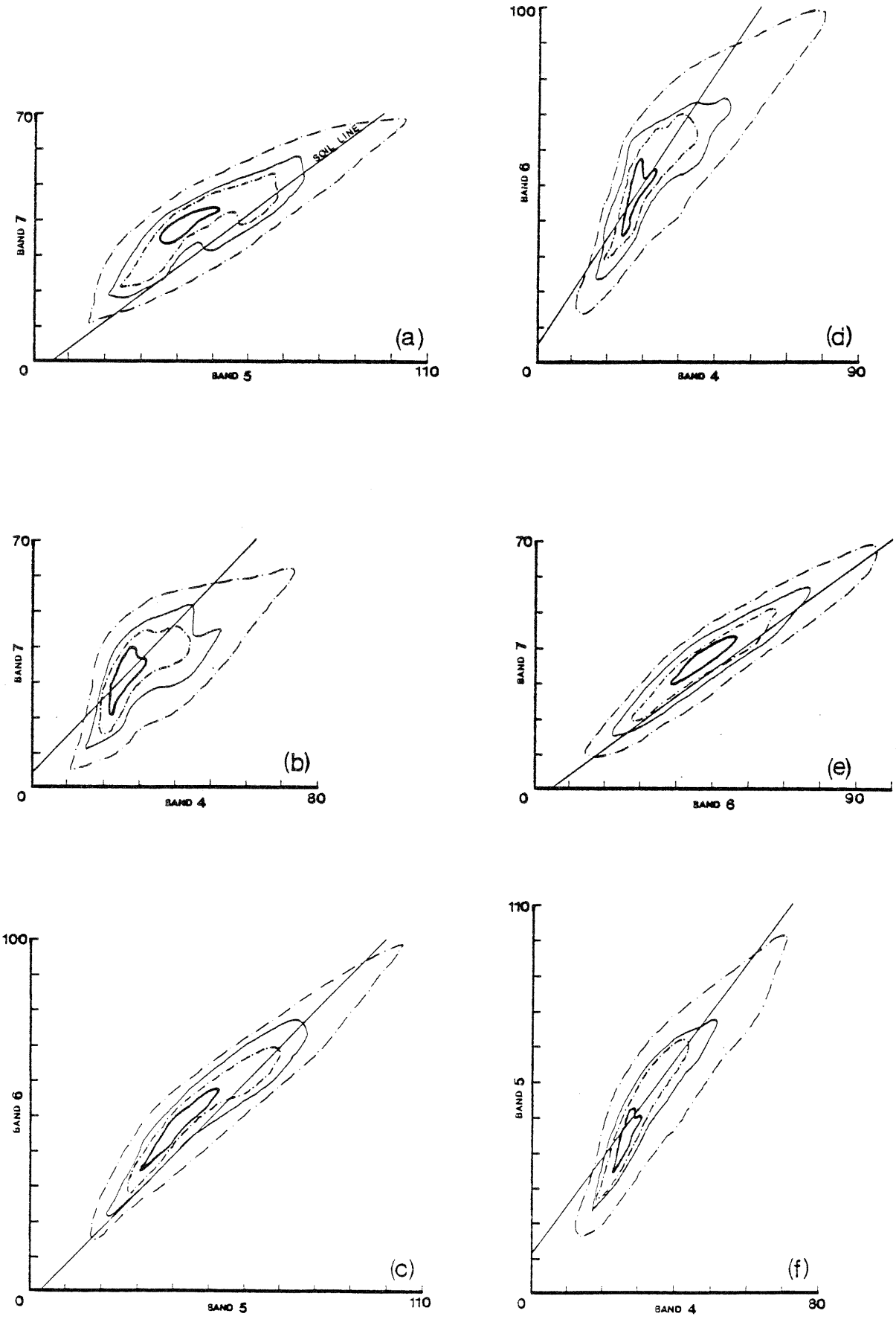

Figure 2. Position of bare soil, non-green and green vegetation 'end points' in #7/#5 Landsat space, showing scatter about mean values.

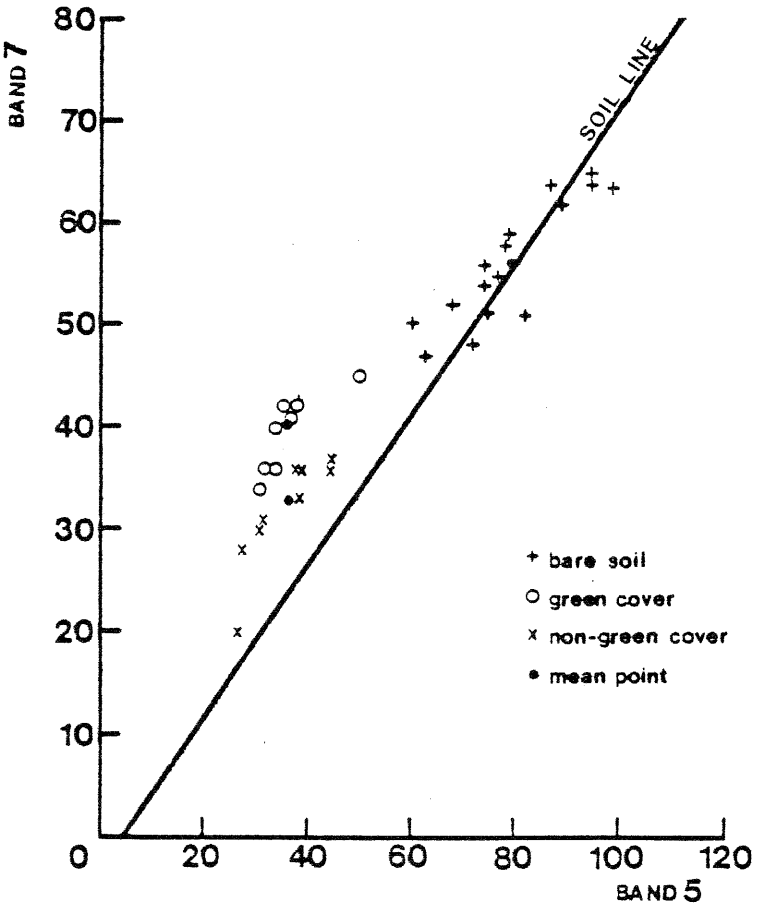

Figure 3. Reflectance of bare soil in #7/#5 Landsat space.

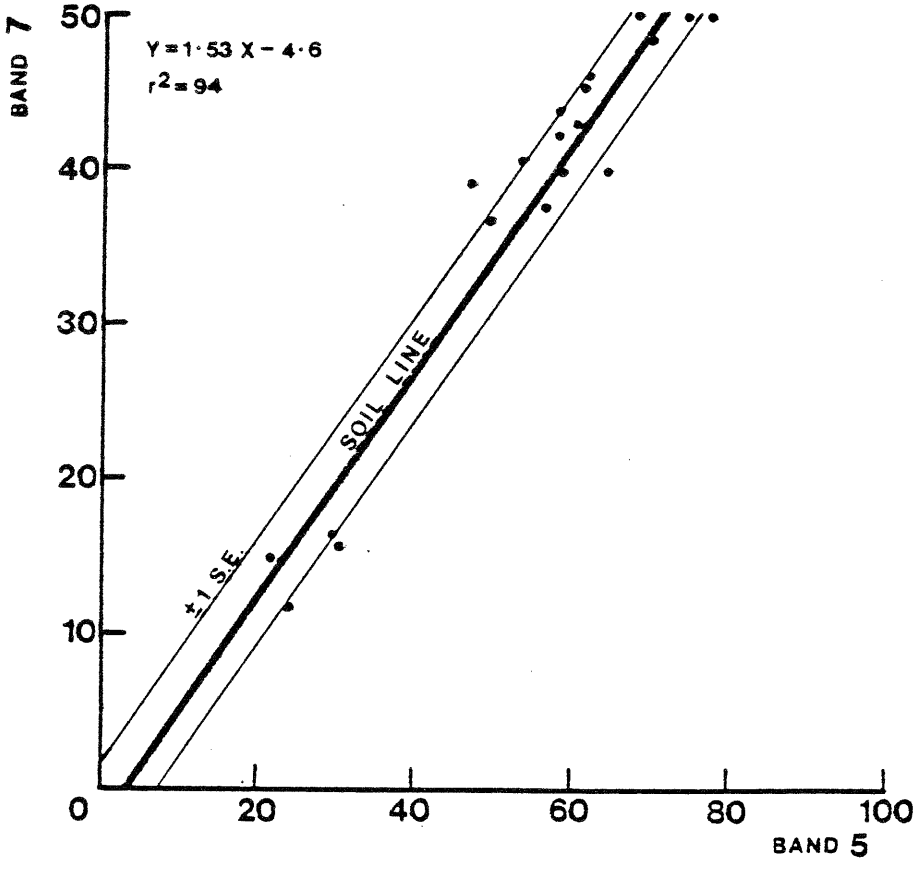

Figure 4. The 3-component model showing vectors to bare soil, non-green and green cover 'end-points'. Plotted points are positions of pixels of high, medium, low and sparse green cover within the triangular distribution.